Structure and Physiology of the Ant Ocelli

Bhavana Penmetcha

Department of Biological Sciences,
Faculty of Science and Engineering
Macquarie University, Sydney NSW Australia

A thesis submitted for the degree of Master of Research

31th May 2019

This thesis is written in the form of a journal article from *Journal of Comparative Physiology A*

Declaration

I wish to acknowledge the following assistance in the research detailed in this report:

Dr. Ajay Narendra and Dr. Yuri Ogawa, my supervisors, for assisting with field work, experimental design and technique, statistics in R and manuscript preparation.

All other research described in this report is my own original work.

This work has not been submitted for a higher degree to any other university or institution.

Bhavana Penmetcha

31th May 2019

Contents

Acknowledgements

This project would not have been possible without the continued guidance and support of my supervisors, Dr. Ajay Narendra and Dr. Yuri Ogawa; both of whom have been patient and encouraging every step of the way. The uplifting and positive encouragement that I received from Ajay lead me through to the completion of this thesis especially in a field like science where one is often faced with unexpected obstacles.

I also thank Yuri, for teaching me the procedures and techniques so diligently. It was comforting to be able to talk to her about the struggles of using a technique such as electrophysiology, which although can be very rewarding can also tend to be a very time-consuming process with low success rates. She has been patient, accepting and extremely helpful throughout this project.

I would not have been able to conduct majority of the experiments in this thesis without the help of Dr. Nathan Hart, Dr. Laura Ryan and all the other members of Dr. Nathan Hart's lab including Olivia, Louise and Anthony. I am very thankful for their generosity and for being so accommodating to me while I utilised the equipment from their lab.

Finally, I would like to thank the other students from the department past and present: Ravi for always listening to my frustrations, complaints and encouraging me to be positive; Theo and Anika for their help with statistics, R and all the fun times we have had together; Zac, Franne, Molly, Ko-Haun and Callum for all the fun excursions and support during this year.

Abstract

Most flying insects possess single lens eyes known as ocelli that assist in flight, navigation and also have an indirect role in foraging. In this thesis, I studied the ocelli of pedestrian ants by characterising the anatomy of the ocelli in three species of desert ants and physiologically measuring the visual properties of the ocelli in day- and night-active *Myrmecia* ants. I found that the Saharan desert ants had a fused rhabdom and anatomical features that would make them polarisation sensitive. The Australian desert ant, *M. bagoti* had an unusual ocellar retina with open rhabdoms wherein each retinula cell contributed microvilli in more than one orientation, making them unlikely to be polarisation detectors. In *Myrmecia*, I measured the contrast sensitivity and spatial resolving power of the ocellar second order neurons. I found that in all species when both the compound eyes and ocelli were exposed to the visual stimuli, the compound eye contributed significantly to the ocellar second order neurons. However, when the compound eyes were occluded the response from the ocellar second order neurons was not quantifiable, which made it difficult to measure the visual properties of the ocelli. I discuss these anatomical and physiological findings in the ecologically relevant conditions that each species encounters.

Keywords: ocelli, ants, polarisation sensitivity, PERG, spatial resolution

Introduction

In addition to compound eyes, flying insects typically possess single lens eyes known as ocelli. In most insects, three single lens eyes are placed in a triangular formation on the dorsal surface of the head (Mizunami 1995). Ocelli, although present in many flying insects, are distinctly absent in most walking insects (Kalmus 1945), with some exceptions such as the Australian ant genus *Myrmecia* and the desert ant species: *Melophorus bagoti*, *Cataglyphis fortis* and *Cataglyphis bicolor*. Due to this, the functions of the ocelli have been largely studied in flying insects. We know from both dragonflies and locusts that the ocelli are especially important to detect the horizon (Stange et al. 2002; Berry et al. 2007b) and to control their head position around the roll and pitch axes during flight. In addition, ocelli play a crucial role in light detection required for flight initiation (Schricker 1965; Wellington 1974; Gould 1975; Eaton et al. 1983; Sprint and Eaton 1987) phototaxis and orientation (Hu and Stark 1980; Wehrhahn 1984; Lazzari et al. 1998). Ocelli can also provide compass information by sensing the pattern of polarised skylight (*Bombus terricola occidentalis* (Wellington 1974), *Cataglyphis bicolor* (Fent and Wehner 1985; Fent 1986)) or some form of a celestial cue (*Melophorus bagoti* (Schwarz et al. 2011b, a)).

A typical ocellus consists of a lens, a vitreous body, an iris, a corneagenous cell layer, a dorsal retina, a ventral retina and a neuropil (Mizunami 1995; Zeil et al. 2014; Narendra et al. 2016; Ribi and Zeil 2017, 2018). The ocellar retina consists of retinula cells that have finger-like projections called microvilli. These finger-like projections together are called rhabdomeres. Two or more retinula cells contribute microvilli to form a rhabdom which is the photosensitive structure. In ants (*Myrmecia* and *Camponotus*), the ocellar rhabdoms in cross-section are wider, shorter and oval-shaped (Narendra et al. 2016; Narendra and Ribi 2017), compared to bees and wasps which are thin and elongated (Toh and Kuwabara 1974; Kral 1979; Ribi et al. 2011; Zeil et al. 2014). The anatomical organization of the rhabdoms can also inform us about the potential for polarization sensitivity (Taylor et al. 2016; Narendra and Ribi 2017; Ogawa et al. 2017; Ribi and Zeil 2018). In hymenopterans, the ocellar rhabdoms that are polarisation sensitive are formed by two opposite retinular cells providing microvilli (Zeil et al. 2014; Ribi and Zeil 2018). In cross-sections, these microvilli are oriented perpendicular to the long axis of the rhabdom and the microvilli are aligned primarily in one direction (Ribi et al. 2011). Ocellar rhabdoms which are not polarisation sensitive tend to be curved (Berry et al. 2011) or tend to be made by retinula cells that contribute microvilli in more than one direction (Narendra and Ribi 2017). *Myrmecia* workers active in low light conditions have evolved distinct ocellar adaptations including larger ocellar lenses and wider rhabdoms compared to their diurnal counterparts (Narendra and Ribi 2017). These adaptations are likely to improve their optical

sensitivity under low light conditions (Wellington 1974). So far, in ants, the anatomical structure of the ocelli has been described only in species where the behavioral function is unknown (e.g., in different species of *Myrmecia* (Narendra and Ribi 2017) and alates of *Camponotus* (Narendra et al. 2016)). Examining the anatomical structure of the ocelli of ants where the behavioral function is known will give us more insight into its functional significance.

The capabilities of an animal's eye is typically characterised by its spatial resolving power which is the ability to discriminate small objects in a scene, and contrast sensitivity which is the ability to differentiate visual stimuli as their contrast decreases (Land 2002). The ocelli in several insects produce under-focused images as their focal plane is located behind the retina (*Locusta migratoria* (Wilson 1978), *Megalopta genalis* (Warrant et al. 2006), *Calliphora erythrocephala* (Cornwell 1955; Schuppe and Hengstenberg 1993), *Euglossa imperialis* (Taylor et al. 2016), *Xylocopa leucothorax* and *Xylocopa tenuiscapa* (Somanathan et al. 2009a)). However, in a few other species the ocelli are capable of resolving images because the plane of best focus is close to the retina (*Apis mellifera* (Ribi et al. 2011; Hung and Ibbotson 2014), *Apoica pallens* and *Polistes occidentalis* (Warrant et al. 2006), *Hemicordulia tau* and *Aeshna mixta* (Berry et al. 2007a, b)). These measures are typically estimates derived from histological techniques. Some physiological experiments have also been carried out in dragonflies and locusts to estimate the ocelli's ability to resolve images (spatial resolution) by calculating the angular sensitivities of the photoreceptors (Wilson 1978; van Kleef et al. 2005). The ability to discriminate contrasts in the ocelli of honeybees (Hung and Ibbotson 2014; Ribi and Zeil 2018) has also been investigated using histological methods. However, to the best of my knowledge definite physiological estimates of the image and contrast discrimination abilities of the ocelli are lacking.

In this study, I first carried out a comparative anatomical analysis of the ocelli of two desert ant species where the ocellar function is known: *Cataglyphis bicolor* (Mote and Wehner 1980; Fent and Wehner 1985) and *Melophorus bagoti* (Schwarz et al. 2011b, a) and one related species, *Cataglyphis fortis,* in which the ocellar function is unknown, but the ants exhibit similar navigational mechanisms as in *C. bicolor* (Penmetcha et al, in review). In the second part of my study, I aimed to quantify the spatial resolving power and contrast sensitivity simultaneously in the ocelli of two primarily nocturnal and two primarily diurnal species of *Myrmecia* ants using pattern electroretinography (PERG) (Porciatti 2007). I could not carry out physiological investigations in the desert ant species as it demanded a continuous supply of a large number of animals that were meant to be alive for a prolonged period of time. This was not possible during my research program. Hence, I used ants from the genus *Myrmecia* which were locally available since closely related species within

this genus are active at different times of the day (Greiner et al. 2007) giving me an opportunity to compare ocellar physiology in day- and night-active ants. *Myrmecia* are large ants (8-30mm in body length) with large ocelli that aid in ease of recording (Narendra et al. 2011; Narendra and Ribi 2017). To compare differences in walking and flying modes of locomotion, I also measured the same properties of the ocelli in a flying insect: *Apis mellifera*. The PERG is a particular kind of ERG that is obtained in response to contrast modulation of patterned visual stimuli at constant mean luminance. The characteristics of the responses are fundamentally different from that of the ERG where the responses are due to flashes of light (Porciatii 2007). The PERG has been used primarily for humans (Bach et al. 2000), birds (Ghim and Hodos 2006), turtles (Armington and Adolph 1990) and sharks (Ryan et al. 2017), and only recently this technique was used to record from the compound eyes of *Myrmecia* ants (Ogawa et al. 2019). Here, I adapted the PERG technique to determine the ability of the ocelli to resolve fine detail and its ability to discriminate between contrasts in its visual field.

Materials and Methods

Study species and collection sites

I investigated the structure of the ocelli in three desert ant species: the central Australian *Melophorus bagoti* and the North African *Cataglyphis bicolor* and *Cataglyphis fortis*. *Melophorus bagoti* was collected from Alice Springs, NT and the two *Cataglyphis* species were collected from Mahres, Tunisia. Live specimens were collected in jars and brought back to the laboratory on a single trip. All three species exhibit considerable size variation and I used the large sized workers for morphometrics and histology (n=5 for each species). Working with these ants requires no ethics approval in Australia.

I studied the physiology of the median ocelli of worker ants of four *Myrmecia* species: diurnal-crepuscular *Myrmecia gulosa* (Sheehan et al. 2019) and *Myrmecia tarsata* (Greiner et al. 2007); and the strictly nocturnal *Myrmecia midas* (Freas et al. 2017) and *Myrmecia pyriformis* (Greiner et al. 2007; Narendra et al. 2010). I also studied the workers of the European honeybee *Apis mellifera*. The animals were captured from the following locations on multiple trips as and when the experiments were underway: *M. midas*, *M. tarsata* and *A. mellifera* from Macquarie University campus, Sydney NSW (33°46'10.24"S, 151°06'39.55"E); *M. gulosa* from Western Sydney University campus, Hawkesbury, Sydney NSW (33°37'46.35"S, 150°46'04.47"E); *M. pyriformis* from The Australian National University campus, Canberra, ACT (35°16'50"S, 149°06'43"E).

Histology

The ocelli of all three desert ant species were fixed in bright light conditions. Ants were immobilised on ice and their mandibles were removed. Optimal fixation was achieved by cutting most of the compound eye and exposing the anterior, posterior and the ventral head capsule. Specimens were fixed for 4 hours at room temperature in a mixture of 2.5% glutaraldehyde and 4% paraformaldehyde in phosphate buffer (pH 7.2 – 7.5). This was followed by a series of buffer washes and post-fixation in 2% OsO_4 in distilled water for one hour at room temperature. Samples were then dehydrated in an ethanol series, transferred to propylene oxide (or acetone) and embedded in Epoxy resin (FLUKA, Sigma-Aldrich, St. Louis, USA). Embedded samples were split to separate the median ocellus and re-embedded. This ensured that the orientation and the correct plane of sectioning could be chosen for the median ocellus. One-micron thick cross-sections were cut on a Leica Ultra microtome (UC7, Leica, Germany) using a diamond knife (Diatome, Pennsylvania, USA). Sections for light microscopy were stained with toluidine blue and digitally photographed in a Zeiss or Leica microscope. Ultra-thin sections (50 nm thick) for transmission electron microscopy were stained with 6% saturated uranyl acetate (25 min) and lead citrate (5 min) before viewing with a FEI Tecnai G2 or Hitachi transmission electron microscope.

For five individuals in each species, I determined the rhabdom diameters from cross-sections taken at the distal one-third of the retina. For reasons that will become apparent in the results, this was not possible to carry out in *M. bagoti*. Ant ocellar rhabdoms varied dramatically in shape. Hence to measure rhabdom diameters I quantified the cross-sectional area of each rhabdom and calculated the diameter of the circle equivalent to this area. I measured the distal to proximal rhabdom length from longitudinal sections along the anterior-posterior plane in the median ocellus. For this, in five individuals for each species, I measured rhabdoms that were completely visible in a single section: *C. fortis*: number of rhabdoms=16; *C. bicolor*: n=13; *M. bagoti*: n=13.

An estimate of the magnitude of polarisation sensitivity of individual receptors can be derived from rhabdom straightness which is correlated to the orientation of the microvilli in cross-sections (Zeil et al. 2014) (Fig. 4c). I measured in one animal for each species, the straightness of all rhabdoms in cross-sections by digitising four equidistant positions along the long axis of each rhabdom using a custom-written software Digilite (© Jan Hemmi & Robert Parker) in Matlab (Mathworks, Nattick, USA). I then determined the rhabdom straightness from the segment orientation (between points 1-2, 1-3) and calculated the difference between the average segment orientation and the absolute orientation (between points 1-4)(Fig. 4c), a method that has been used to analyse ocellar rhabdoms

straightness in honeybees (Ribi et al. 2011) and in ants (Narendra et al. 2016; Narendra and Ribi 2017). I also determined the global organisation of rhabdom orientations in the median ocellus. These measures were not possible to carry out in *M. bagoti* as will be explained in the results.

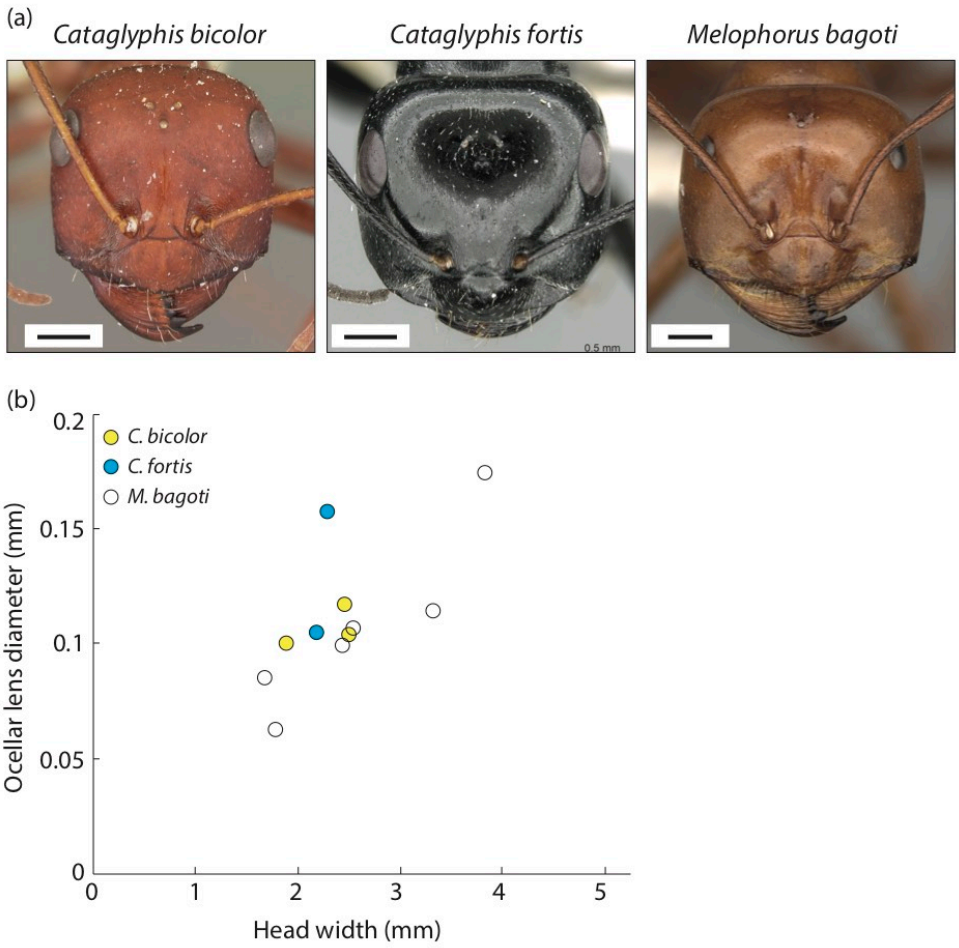

Figure 1. External morphology of ocelli in three species of desert ants. (a) Dorsal view of the head and position of the ocelli in *Cataglyphis bicolor*, *Cataglyphis fortis* and *Melophorus bagoti* (www.antweb.org). Scale bar=0.5mm. (b) Relation between median ocellar lens diameter and head width in the three species. Data is derived from specimen images available on Antweb. From Penmetcha et al., in review.

Table 1. Properties of the median ocellus in three desert ant species.

	Cataglyphis bicolor n=5	*Cataglyphis fortis* n=5	*Melophorus bagoti* n=5
Lens diameter (μm) (Mean ± S.E.)	48.60±0.27	37.95±0.16	67.03±0.43
Rhabdom area in cross section (μm^2) (Mean ± S.E.)	0.50±0.01	0.65±0.02	-
Rhabdom width in cross section (μm) (Mean ± S.E.)	0.16±.005	0.21±.008	-
Rhabdom length in longitudinal section (μm) (Mean ± S.E.)	D: 20.15±0.43 V: 7.48±1.06	D: 15.96±1.95 V: 5.86±0.37	D: 18.26±1.53 V: 6.86±0.83

Rhabdom length in dorsal (D) and ventral (V) retina are shown.

Ocellar diameter and head width

For the desert ant species, I measured head width which is often used as a proxy for body size in ants (Weiser and Kaspari 2006) and the external diameter of the median ocellus using Fiji (Schindelin et al. 2012) from all available specimens on Antweb (antweb.org).

For each individual in each *Myrmecia* species, I captured images of the dorsal head surface and a magnified view of the ocelli in the same orientation using a stereomicroscope (Leica M205FA, Camera Leica DFC 550, Leica Microsystems, Germany). All five species had one median ocellus and two lateral ocelli. For this study I focused my attention on the median ocellus. I measured head width and the external diameter of the median ocellus using Fiji (Schindelin et al. 2012).

Pattern electroretinography (PERG)

Ants were kept on ice for 5-10 mins to anesthetize them before removing their antennae, legs and gaster. Each animal was then fixed horizontally onto a plastic stage with its dorsal side facing upwards

using beeswax. The same was done with the honeybees after anesthetizing and removing their wings and legs. In ants, the orientation of the median ocelli varied slightly between species (Narendra and Ribi 2017). For example, in *M. midas* and *M. pyriformis* the median ocelli was upward-facing, whereas in *M. tarsata* and *M. gulosa* the median ocellus was forward-facing. Hence, I tilted the head slightly to ensure the median ocellus received the stimuli. In order to place an active electrode on the ocellar retina in ants, I made a small incision using a sharp blade and thinned the cuticle, immediately posterior to the median ocellar lens. Vaseline (Unilever, USA) was placed on the thinned cuticle to prevent dehydration and a layer of conductive gel (Livingstone International Pty Ltd., New South Wales, Australia) was added. In the honeybee, the hair around the median ocellus was removed using sharp forceps (Dumont, ProSciTech, Queensland, Australia) for easier access and placement of electrode.

The animals were then mounted within a Faraday cage to record the spatial resolving power and the contrast sensitivity of their ocellar second order neurons (Fig. 2). An active electrode of platinum wire of 0.25mm diameter with a sharp tip was placed at the point of incision, posterior to the median ocellar lens in the case of ants. In honeybees, the active electrode was placed on the cuticle, posterior to the median ocellar lens. The active electrode in both cases was immersed in the conductive gel. A silver/silver-chloride wire of 0.1mm diameter was inserted into the mesosoma and served as an indifferent electrode.

The ERGs were filtered between 0.1 – 100Hz and amplified at 1k gain using a differential amplifier (DAM50, World Precision Instruments Inc., FL, USA), which was connected to a computer via a 16-bit analog-to-digital converter device (USB-6353, National Instruments, Austin, TX, USA)(Fig. 2). The data was acquired at 5k Hz sampling rate using a custom-built acquisition program on Visual Studio (2013, Microsoft Corporation, Redmond, WA, US). All experiments were performed in a dark room at room temperature (21-25 °C). To exclude any effects of the circadian rhythms on eye physiology, the experiments were conducted at each species' typical activity time, i.e. from 1-6 hours post-sunset for nocturnal species and 2-8 hours post-sunrise for the primarily diurnal species.

The PERG visual stimuli was projected by a digital light processing projector (W1210ST, BenQ corporation, Taipei, Taiwan) onto a white screen (W51 x H81cm) at a distance of 30 cm from the animal. The stimuli were vertical contrast-reversal sinusoidal gratings of different spatial frequencies (cpd: cycles per degree) and Michelson's contrasts (Fig. 2). They were generated using Psychtoolbox 3 (Pelli, 1997) and MATLAB (R2015b, Mathworks, Natick, MA, US) and controlled

via a custom Visual Basic Software written in Visual Studio (2013, Microsoft Corporation, Redmond, WA, US). The mean irradiance of the grating stimulus was 1.75 x 10^{-4} W/cm^2 which was measured using a calibrated radiometer (ILT1700, International Light Technologies, Peabody, MA, US). A temporal frequency of 4 Hz was used for all the stimuli.

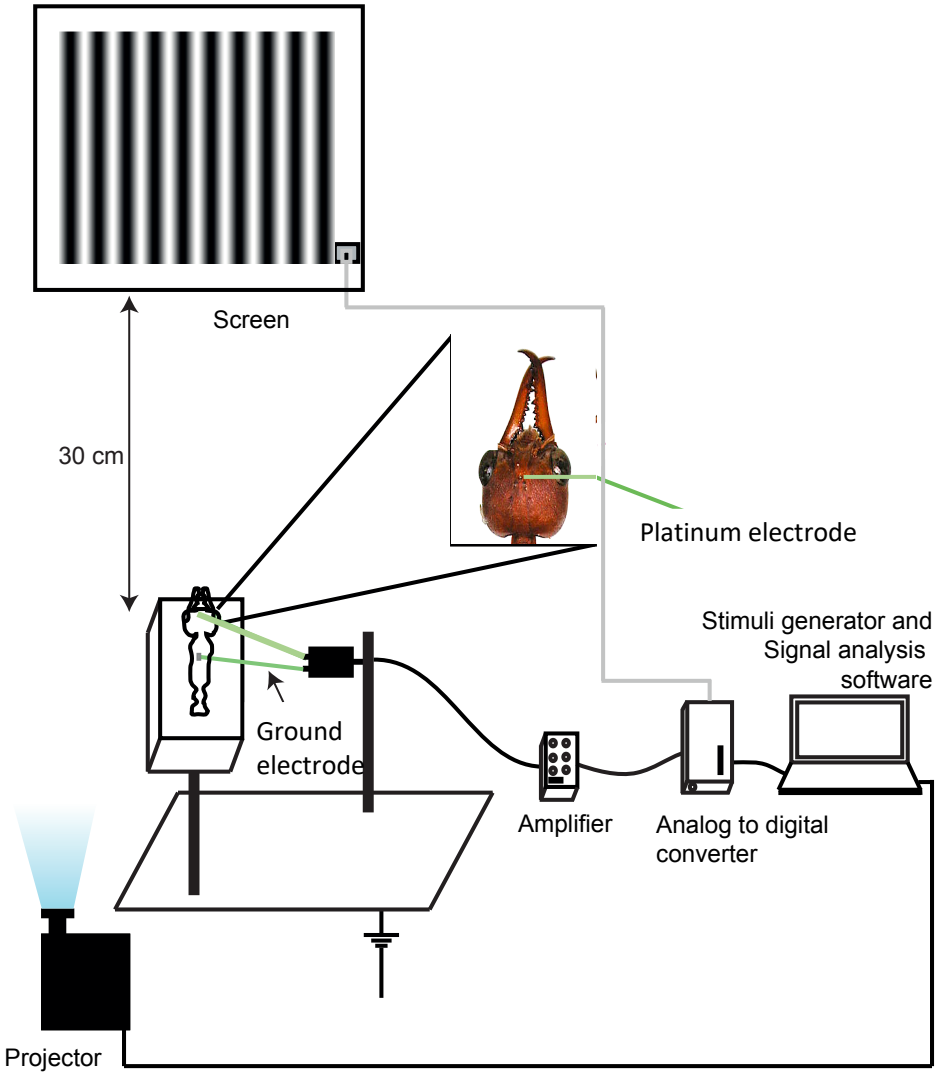

Figure 2. Schematic of the pattern electroretinography set-up. An ant was mounted on a plastic stage 30 cms from the screen on to which the vertical contrast-reversal sinusoidal gratings were projected as the stimuli. Electrical activity was recorded by placing a platinum electrode on the retina of the median ocelli while the ocelli were exposed to the stimuli. The photodiode present on the screen was used to sync the stimulus to the response. Modified from Palavalli-Nettimi et al 2019.

Prior to the first recording the animal was adapted to a uniform grey stimulus with the same mean irradiance as the grating stimuli for 20 minutes. To measure the contrast sensitivity function of the animals, 9 spatial frequencies (0.05, 0.1, 0.15, 0.2, 0.26, 0.31, 0.36, 0.41, 0.52 cpd) and upto five

contrasts (95%, 50%, 25%, 12.5%, 6%) for each spatial frequency was presented. The spatial frequencies were first presented in decreasing order of frequencies (0.52, 0.36, 0.26, 0.15, 0.05 cpd), skipping one frequency in between. In order to evaluate any degradation in response over time the interleaved frequencies were then presented in ascending order (0.1, 0.2, 0.31, 0.41 cpd). At each spatial frequency, all five contrasts were tested in decreasing order. Each combination of the stimuli was recorded for fifteen repeats, five seconds each and averaged in the time domain. The averaged responses were then analysed using a Fast Fourier Transform (FFT). The non-visual electrical signal (background noise) was recorded at 2 spatial frequencies (0.05 and 0.1 cpd) at 95% contrast with a black board to shield the animal from the visual stimuli before and after running the experimental series. The maximum signal out of four control runs was used as the noise threshold.

Spatial resolution and contrast threshold

An F-test was used to access whether the response signal at the second harmonic (8 Hz) of the FFT response spectrum, for each spatial frequency and contrast combination, was significantly different from ten neighbouring frequencies, five on either side. The spatial resolving power and contrast threshold was calculated by interpolating the last point above the noise threshold whose amplitude at 8Hz was also significantly greater than the 10 surrounding frequencies, and the first point below the noise threshold. If the first point below the noise threshold was not significantly greater than the 10 surrounding frequencies, the last point above the threshold was considered as the spatial resolving power, without interpolating between two data points. As the spatial frequency of the visual stimuli increases the amplitude of the PERG response at the second harmonic decreases. The point at which the PERG response amplitude dropped below the noise threshold was defined as the spatial resolving power at the highest contrast. At each spatial frequency of the visual stimuli, the amplitude of the PERG response decreased with decreasing contrast. The point at which the amplitude dropped below the noise threshold was taken as the contrast threshold. The contrast threshold at each spatial frequency of gratings was used to calculate the contrast sensitivity at that particular spatial frequency using the formula: 1/contrast threshold.

Assessment of the contribution of the compound eyes to ocellar second order neurons

Using the PERG method I placed the electrode immediately posterior to the ocellar lens and recorded from neurons that responded to both light and dark gratings of the visual stimuli. These were most likely the ocellar second-order neurons (Palavalli-Nettimi et al 2019) (which includes input from the lateral ocelli as well (Hung and Ibbotson 2014; Wilby et al. 2018)). To identify the contribution of the compound eyes to the ocellar second-order neurons, I performed the PERG on three animals each in the nocturnal *M. midas*, the diurnal-crepuscular *M. tarsata* and European honeybee *A. mellifera*

with the compound eye covered with black nail enamel (B Beauty, NSW, Australia) such that the visual stimulus could only be received by the ocellar lens. In the honeybees, I used black tape (Nichiban, Tokyo, Japan) as the black nail enamel interfered with the recordings.

Statistics

I tested whether the maximum contrast sensitivity and the spatial resolving power differed between the five species using a linear model in RStudio (Version 1.1.463, RStudio, Inc. Boston, MA, US). I used a linear-mixed effects model to assess the effect of species, spatial frequency of stimulus and locomotion on the contrast sensitivity function using a maximum likelihood (ML) estimation method. I also did the same, among ants, to assess the effect of time of activity on the contrast sensitivity functions. This was carried out in the *lme4* package of R (https://cran.r-project.org/web/packages/lme4/index.html). Time of activity in ants, spatial frequency and locomotion were used as fixed effects and animal identity nested within species was used as a random effect. The significances of the fixed effect terms were examined using the t-test with Satterthwaite approximation for degree of freedom (ImerTest package). To test whether the species had an effect on the contrast sensitivity function, I performed an R analysis of variance (RANOVA). The contrast sensitivity and spatial frequency data was log-transformed before the data analysis.

Prior to testing whether the contrast sensitivity functions differed between the two recording sites (ocellar second order neurons and lamina) among species, I confirmed that the recording site had a larger affect among specific species than between species by performing an analysis of variance (ANOVA) with a linear mixed-effects model in R. To identify the species that have differences in the contrast sensitivity functions between the recording sites, I used a Tukey post hoc test implemented in the multicomp package of R. For the spatial resolving power, I confirmed the effect of recording site on the spatial resolving power by performing ANOVA with a linear model in R. Similar to the method adopted above, I used a Tukey post hoc test to identify the species that have differences in spatial resolving powers between the two recording sites.

Results

Anatomy

All three species of desert ants had three ocelli: a median ocellus and two lateral ocelli organised in a triangular shape on the dorsal surface of the head (Fig. 1, Table. 1). Even in a limited sample size,

the trend of the median ocellar lens increasing with body size in all three species was distinct (Fig. 1b). The median ocellar lens in all species were smooth and convex in shape.

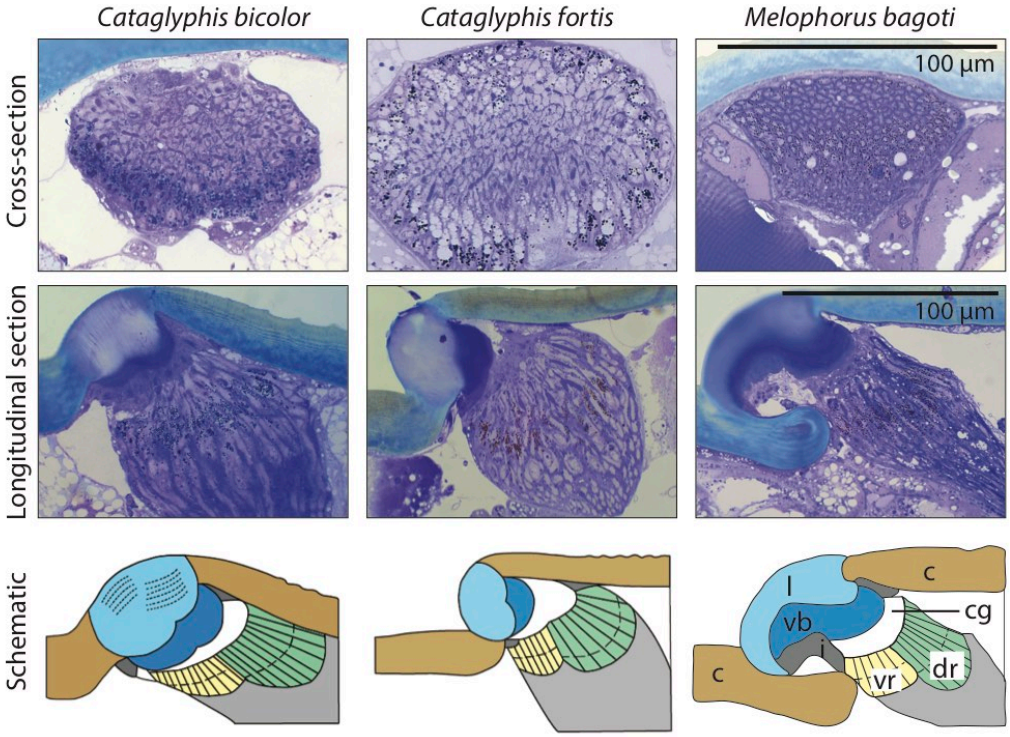

Figure 3. Structure of the median ocellus of three desert ant species. Top row: cross-section, bottom panel: longitudinal section of the median ocellus showing different optical components: c, cuticle; l, lens; cg, corneagenous layer; vb, vitreous body; i, iris; vr, ventral retina looking at the sky; dr, dorsal retina looking at the horizon. Scale bar for top and bottom panels are shown in panels of *M. bagoti*. From Penmetcha et al., in review

Proximal to the lens was a vitreous body followed by a corneageneous cell layer that produces corneal lens during development. Below this, lies the bipartite retina that was distinct in all three species (Fig. 3, see longitudinal section): the dorsal retina which appears to face the horizon and the ventral retina that appears to face the sky (Fig. 3). In all three species, the distal–proximal length of the rhabdoms in the dorsal retina was nearly thrice that of the rhabdoms in the ventral retina (Table.1).

In cross-sections, the shape of the ocellar rhabdoms of all three species varied greatly from being straight, oblong, circular to having odd geometries. The size of the rhabdoms in cross-sections in both *Cataglyphis* species exhibited little variation (Fig. 3; Table. 1) but were smaller compared to *Myrmecia* ants (Narendra and Ribi 2017). In most flying Hymenopterans, the global orientation of ocellar rhabdoms is consistent (Zeil et al. 2014; Ribi and Zeil 2018). In both *Cataglyphis* species of ants, the ocellar rhabdom orientation had a wide distribution (Fig. 4a). The rhabdoms in *Cataglyphis* species were relatively straight, which is crucial for polarisation sensitivity (Fig. 4b).

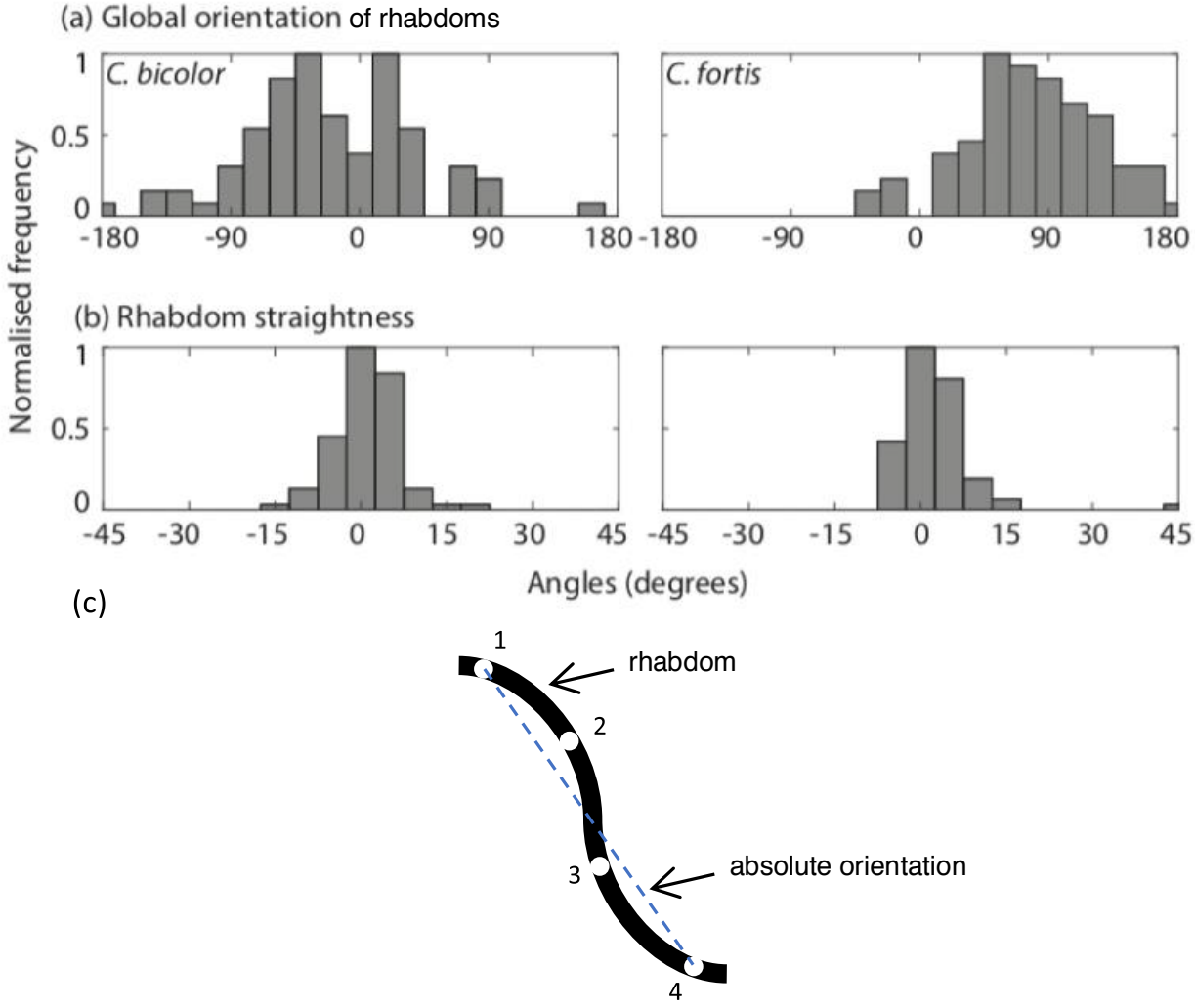

Figure 4. Histograms showing frequency distribution of (a) global orientation and (b) rhabdom straightness in the median ocellus of *Cataglyphis* ants. Global orientation shows the distribution of the orientation of the rhabdoms in cross-sections, relative to the horizontal (0 deg). For rhabdom straightness, 0 deg indicates least deviation from a straight line. **(c)** Schematic of a single twisting rhabdom with four equidistant points to calculate rhabdom straightness. Dotted line between points 1- 4 indicates absolute orientation. From Penmetcha et al., in review

In flying Hymenopterans, ocellar rhabdoms are fused and typically composed of two paired retinula cells that contribute microvilli perpendicularly to the long axis of the rhabdom – this allows animals to compare e-vector intensities (Zeil et al. 2014). Such a pattern was seen in *C. bicolor* (Fig. 5, Fig. 6). The related *C. fortis* also had fused rhabdoms but they were composed of 2-4 retinula cells (rhabdom in blue in Fig. 5; Fig. 6). Majority of the rhabdoms in *C. fortis* were in the shape of 'T', in which the third or the fourth retinula cell contributed microvilli perpendicular to the microvillar orientation of the other retinular cells, which is characteristic of polarisation detectors. But in some cases (rhabdom shown in red for *C. fortis* and *M. bagoti* in Fig. 5; Fig. 6), retinula cells contributed microvilli in more than one orientation, making these cells less likely to be polarisation sensitive. The most unusual organisation of ocellar retina was in *M. bagoti*, where the rhabdomeres within each

retinula cell were arranged in a hexagonal or a pentagonal shaped network forming an open rhabdom (Fig. 5, Fig. 6). Hence the rhabdom diameter, orientation and straightness in *M. bagoti* could not be measured. Each retinula cell contributed microvilli in multiple orientations making them less likely to be polarisation sensitive. Each retinula cell was separated from the adjacent cell by an intracellular space (Fig. 6) similar to that seen in Dipterans (Toh et al. 1971; Wunderer et al. 1988; Ribi and Zeil 2018).

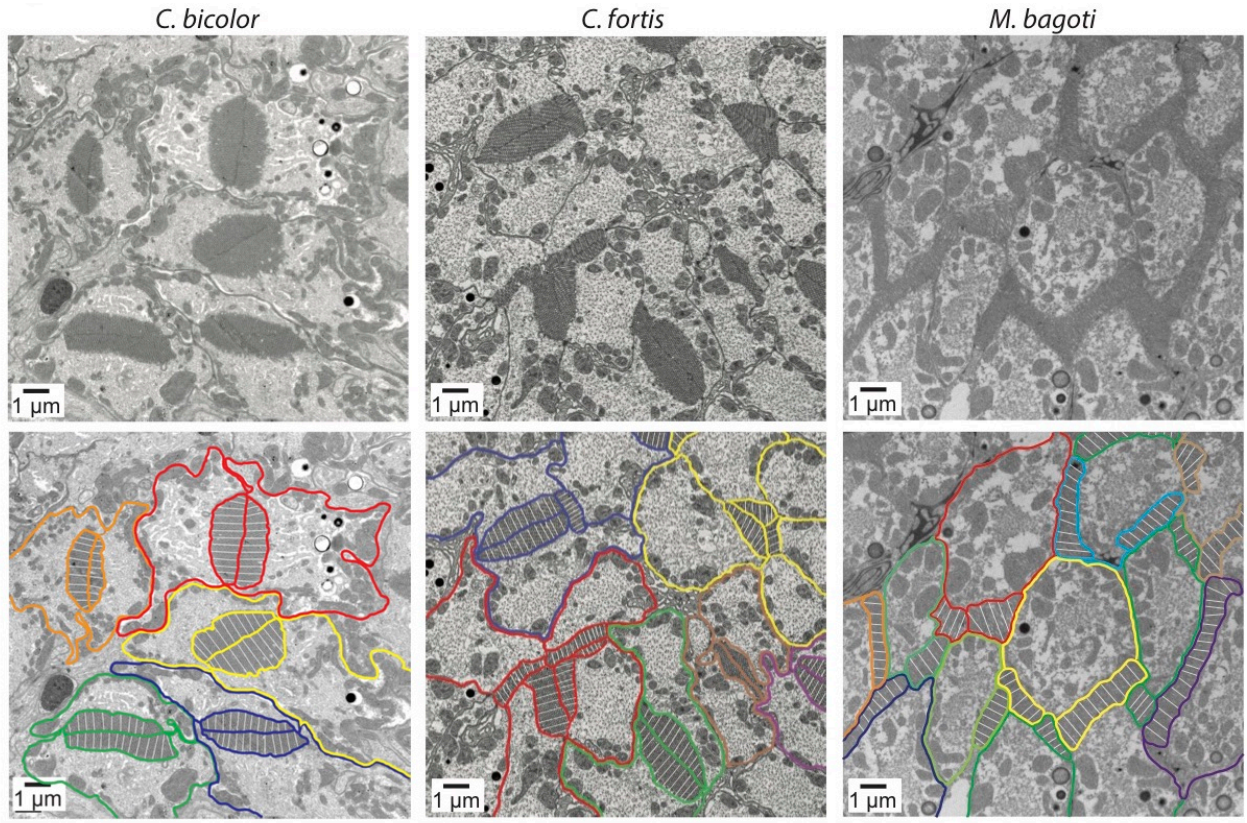

Figure 5. Transmission electron micrographs of median ocellar rhabdom cross-sections in workers of three species of desert ants. Bottom panel: shows retinula cells boundaries and white lines indicate orientation of the microvilli. From Penmetcha et al., in review

Physiology

Contrast sensitivity and spatial resolving power of ocellar second order neurons when both compound eyes and ocelli were exposed to the visual stimuli

Contrast sensitivity

I measured the contrast sensitivity function of the ocellar second order neurons in four species of ants and in the honeybee with both the compound eyes and the ocelli exposed to the visual stimuli (E^+O^+; Table 2). In all five species, at each spatial frequency of the visual stimuli, the amplitude of the PERG

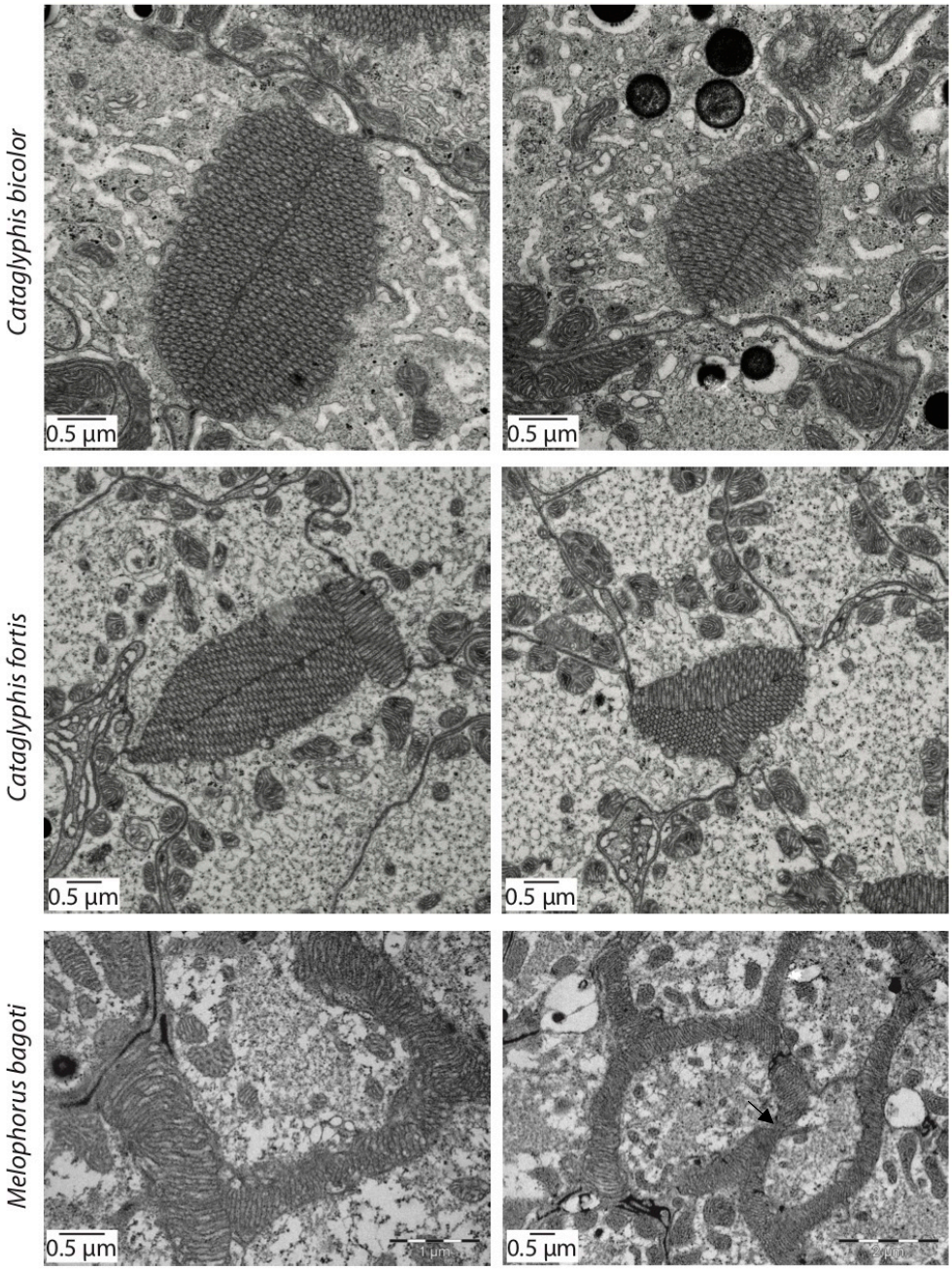

Figure 6. High magnification transmission electron micrographs of median ocellar rhabdom of the three species of desert ants. Top row: *Cataglyphis bicolor*; Mid-row: *Cataglyphis fortis*; Bottom rom: *Melophorus bagoti*. Arrow indicates intracellular space. From Penmetcha et al., in review

response decreased with decreasing contrast. The contrast sensitivity (1/contrast threshold) decreased as the spatial frequency increased in all species (Fig. 7a). The maximum contrast sensitivity was attained at the lowest spatial frequency (0.05cpd) in all five species. The maximum contrast sensitivity did not differ significantly between the five species (Table 3). Among these species, the maximum contrast sensitivity was highest in *M. midas* and lowest in the flying *A. mellifera* (Table 2).

Table 2. Summary of spatial resolving power and maximum contrast sensitivity of ocellar second order neurons of *Myrmecia* ants and *A. mellifera* when both ocelli and compound eyes are exposed to the visual stimuli.

	nocturnal		diurnal-crepuscular		diurnal
	M. midas (n=5)	*M. pyriformis* (n=5)	*M. gulosa* (n=4)	*M. tarsata* (n=5)	*A. mellifera* (n=5)
Head width (mm) (mean ± SE)	3.96 ± 0.24	4.59 ± 0.11	4.08 ± 0.08	3.86 ± 0.11	3.7 ± 0.02
Ocelli diameter (μm) (mean ± SE)	172.95±14.22	202.98 ± 4.4	173.02 ± 2.25	156.08 ± 8.46	286 ± 0.004
Ocelli diameter /Head Width	0.043	0.044	0.042	0.04	0.077
Spatial resolving power (cpd) (mean ± SE)	0.30 ± 0.04	0.25 ± 0.05	0.34 ± 0.02	0.29 ± 0.02	0.26 ± 0.03
Maximum contrast sensitivity	16 (6.3%)	11 (9.1%)	12 (8.3 %)	12.9 (7.7%)	9.2(10.8%)

The contrast sensitivity functions were significantly different between species (p-value = 0.04). Differences in locomotion (walking *vs* flying) between the species did not explain the variation in the contrast sensitivity functions (Table 4). Among ants, the difference in their time of activity also did not explain the variation in the contrast sensitivity functions (Table 5).

Spatial resolving power

The spatial resolving power of the ocellar second order neurons in the five species was measured when both the compound eyes and the ocelli were exposed to the visual stimuli (E^+O^+; Fig. 7b). The spatial resolving power was not significantly different between species (Table 6). Among the five species, *M. pyriformis* had the lowest spatial resolving power and *M. gulosa* had the highest (Table 2).

Compound eye contribution to the ocellar second order neurons

To identify the contribution of compound eyes to ocellar second order neurons, I measured the response amplitude of the PERG from the ocellar second order neurons of *M. midas*, *M. tarsata* and *A. mellifera* for each spatial frequency at 95% contrast. For this I used animals in which: (i) both compound eyes and ocelli were exposed to the visual stimuli (E^+O^+; Fig. 8, left column), (ii) compound eyes were occluded and only ocelli were exposed to the visual stimuli (E^-O^+; Fig. 8, right column). The response amplitude in all three species was significantly lower among individuals whose compound eyes were occluded (E^-O^+; Fig. 8, right column) compared to those in which both the compound eyes and ocelli were exposed (E^+O^+; Fig. 8, left column).

Table 3. Summary of linear model for testing relationship between maximum contrast sensitivity and species. Model: Maximum contrast sensitivity ~ species

Parameter	Estimate	Standard Error	*t*-value	*p*-value
Intercept	1.21	0.09	13.20	<0.001
species	-0.04	0.03	-1.58	0.13

Maximum contrast sensitivity = -0.04**species* + 1.21.

Table 4. Summary of the linear mixed-effects model for testing the relationship between contrast sensitivity function of the ocellar second order neurons, spatial frequency and locomotion in *Myrmecia* ants and *Apis mellifera*. Model: contrast sensitivity ~ spatial frequency + locomotion + (1|species/animal ID). The *t*-tests for fixed effects use Satterthwaite approximations to degrees of freedom (*df*). The variance of each of the random effects is <1.3%

Parameter	Estimate	Standard Error	*df*	*t*-value	*p*-value
Intercept	-0.54	0.13	3.69	-4.0	0.02
Spatial frequency	-1.24	0.06	106.09	-21.59	<0.001
Locomotion	0.03	0.14	2.9	0.18	0.87

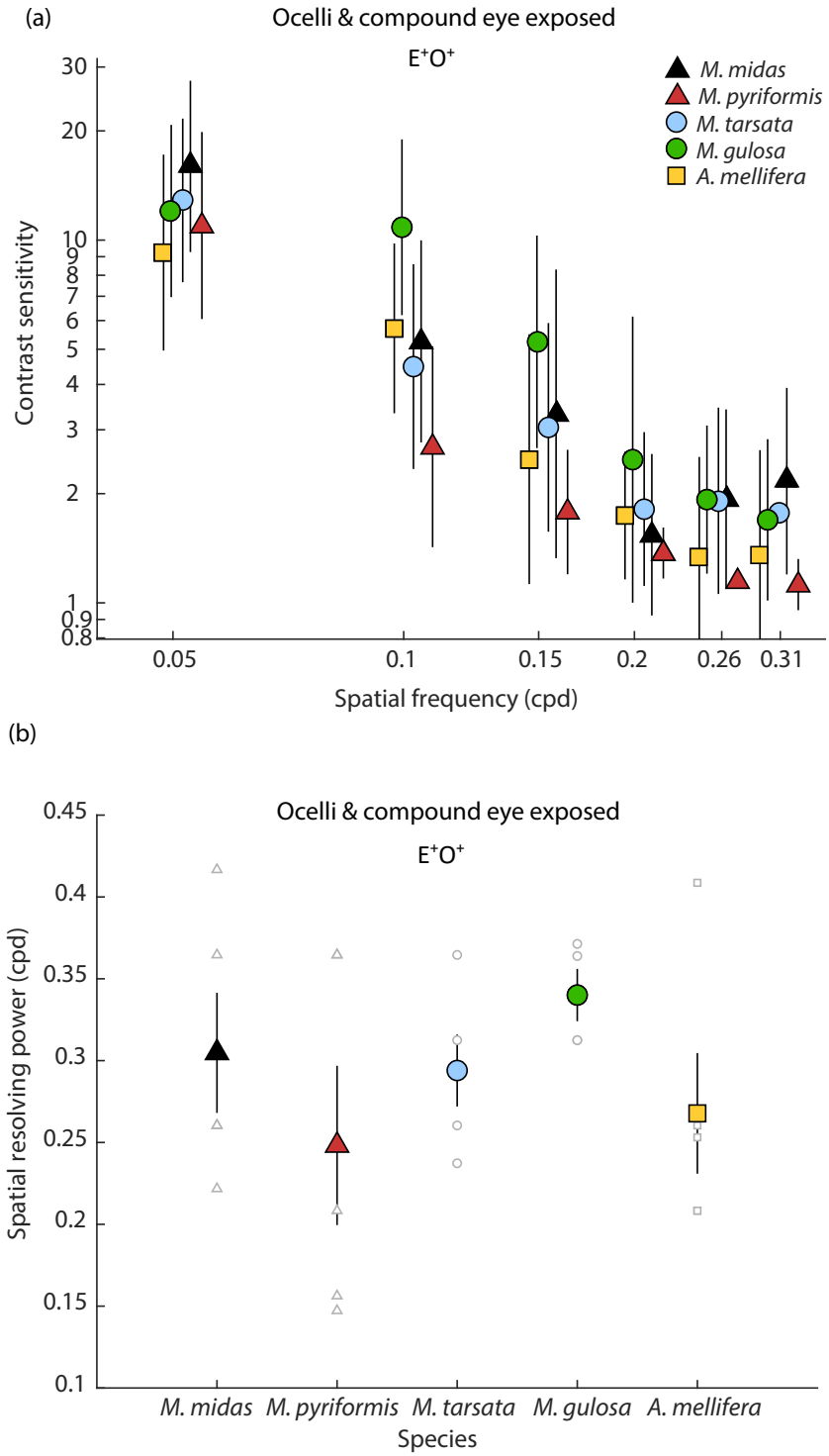

Figure 7. Contrast sensitivity function and spatial resolving power of ocellar second order neurons for *A. mellifera* and for four *Myrmecia* species with both compound eye and ocelli exposed to the visual stimuli. (a) Each data point is the mean contrast sensitivity of all individuals of a particular species at the corresponding spatial frequency. The error bars show 95% confidence intervals. Data points for each species were shifted to the right or left of the recorded spatial frequency to improve visualisation. **(b)** Each coloured data point is the mean spatial resolving power of all individuals of a particular species at 95% contrast. Error bars show standard error. Grey outlined data points are individuals of a particular species. Circles indicate diurnal-crepuscular ant species. Triangles indicate nocturnal ant species. (n=4 for *M. gulosa*, n=5 for remaining species)

Table 5. Summary of the linear mixed-effects model for testing the relationship between contrast sensitivity function of the ocellar second order neurons and time of activity in *Myrmecia* ants. Model: contrast sensitivity ~ spatial frequency + time of activity + (1|species/animal ID). The *t*-tests for fixed effects use Satterthwaite approximations to degrees of freedom (*df*). The variance of each of the random effects is <1.2%.

Parameter	Estimate	Standard Error	*df*	*t*-value	*p*-value
Intercept	-0.53	0.09	4.6	-6.0	<0.01
Spatial frequency	-1.24	0.06	85.9	-19.76	<0.001
Time of activity	-0.05	0.1	1.99	-0.5	0.66

Table 6. Summary of the linear model for testing the relationship between spatial resolving power of the ocellar second order neurons and species in *Myrmecia* ants and *Apis mellifera*. Model: Spatial resolving power ~ species

Parameter	Estimate	Standard Error	*t*-value	*p*-value
Intercept	0.27	0.04	7.19	<0.001
species	0.007	0.01	0.64	0.13

Spatial resolving power = 0.007**species* + 0.27.

Table 7. Results of the ANOVA for testing the effect of spatial frequency of gratings, recording site (ocellar second order neurons and lamina) and species on contrast sensitivity functions in *M. midas*, *M. tarsata*, and *A. mellifera*. Model: contrast sensitivity ~ spatial frequency + recording site + species + (1|animal ID).

Parameter	*df*	*F*-value	*p*-value
Intercept	203	538.3604	<0.001
Spatial frequencies	203	1317.7262	<0.001
Recording site	26	32.7274	<0.001
Species	26	1.2282	0.3093

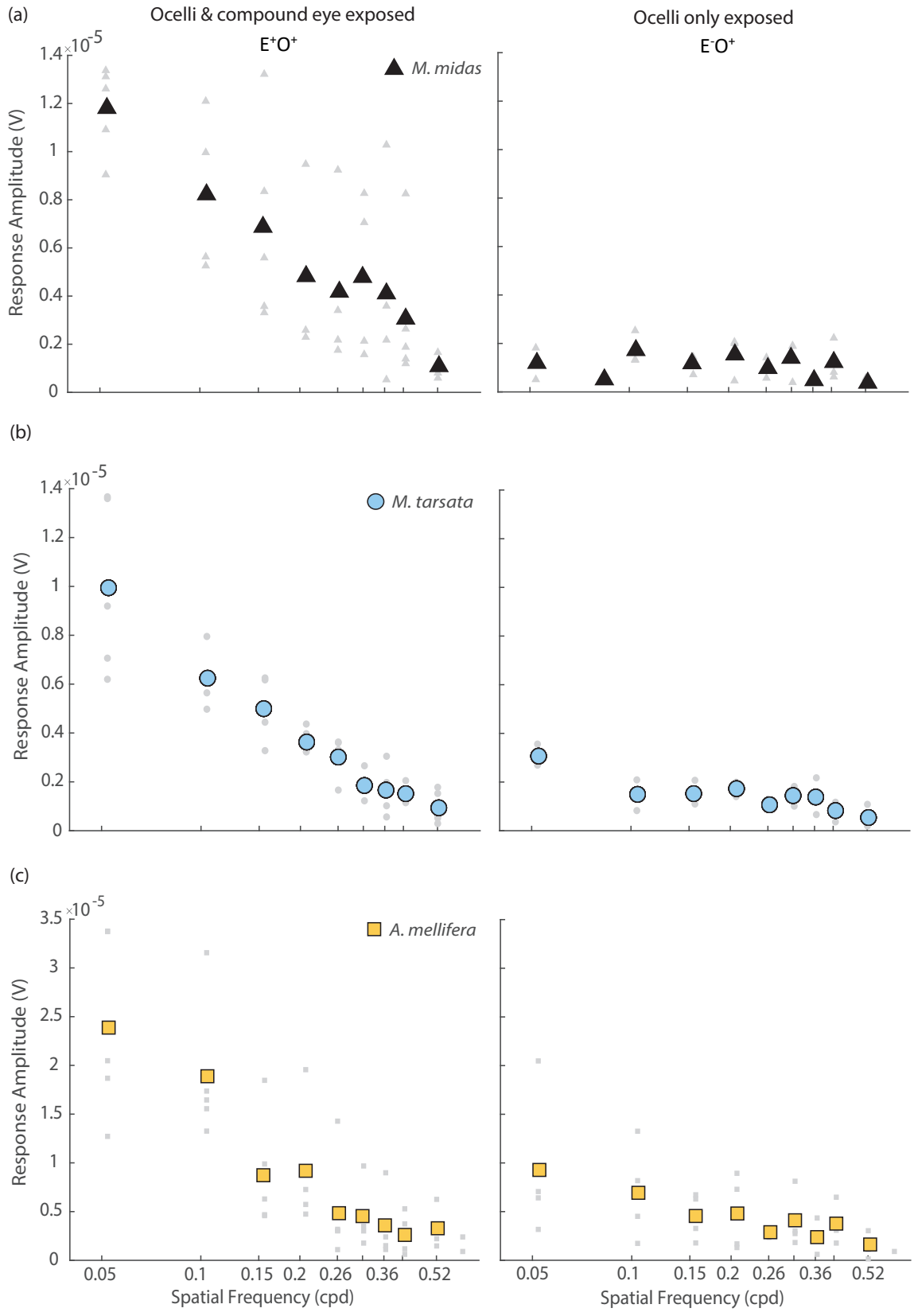

Figure 8. Compound eyes contribution to the ocellar second order neurons in *M. midas*, *M. tarsata* and *A. mellifera*. Left column: both compound eyes and the ocelli were exposed to the visual stimuli (n=5 for each species). Right column: compound eyes were occluded and only the ocelli were exposed to the visual stimuli (n=3 for each species). Amplitude of response signal from the ocellar second order neurons are shown for (**a**) *M. midas,* (**b**) *M. tarsata* and **(c)** *A. mellifera.* Each coloured

data point is the mean amplitude of the signal of all individuals at the corresponding spatial frequency at 95% contrast. Grey data points indicate individuals within the species.

Table 8. Summary of the linear model for testing the relationship between spatial resolving power and recording site (ocellar second order neurons and lamina) in *M. midas*, *M. tarsata,* and *A. mellifera*. Model: spatial resolving power ~ recording site

Parameter	Estimate	Standard Error	*t*-value	*p*-value
Intercept	0.01	0.03	0.28	0.78
Recording site	0.28	0.02	13.68	<0.001

Discussion

This study consists of two parts: first, a comparative anatomical analysis of the desert ant ocelli where I found that, the anatomical data from *C. bicolor* was consistent with the behavioural (Fent and Wehner 1985; Fent 1986) and physiological evidence (Mote and Wehner 1980), suggesting that their ocelli are polarisation sensitive. I also found that the ocelli of *C. fortis* has the possibility for polarisation sensitivity, but this was not the case in the ocelli of *M. bagoti*. In the second part of my study, I aimed to measure the contrast sensitivity and spatial resolving power of ocelli by recording from the ocellar second order neurons using the PERG technique. I found that the response from the ocellar second order neurons was quite low when the compound eyes were covered, which suggests that the compound eyes may contribute significantly to the ocellar second order neurons. Hence, even though the ocellar spatial properties could not be measured in this study, I discuss the implications of my findings.

Anatomy

I first characterised the anatomical structure of the ocelli in three species of desert ants, *Cataglyphis bicolor*, *Cataglyphis fortis* and *Melophorus bagoti.* These species being strictly diurnal had relatively similar and smaller lenses and narrower rhabdoms (in *Cataglyphis* spp) compared to the nocturnal *Myrmecia* ants (Narendra and Ribi 2017). Nocturnal insects tend to have larger ocellar lenses and wider ocellar rhabdoms (Warrant et al. 2006; Somanathan et al. 2009b; Narendra et al. 2011; Narendra and Ribi 2017) in order to improve their optical sensitivity (Horridge 1977).

The organisation of the ocellar retina in the three desert ant species in this study was strikingly different from that of the other species of ants that have been previously studied. In the *Myrmecia* worker ants the rhabdoms were composed of more than three retinular cells and in the nocturnal ants

the retinular cells contributed microvilli in multiple orientations thus destroying polarisation sensitivity (Narendra and Ribi 2017). However, in *C. bicolor* the microvilli were oriented perpendicular to the long axis of the rhabdom (Fig. 5; Fig. 6) indicating that their ocelli are likely polarisation sensitive which supports behavioural (Fent and Wehner 1985; Fent 1986) and physiological evidence (Mote and Wehner 1980). *C. bicolor* nests in both saltpans and around urban regions, whereas its related species *C. fortis* nests exclusively in saltpan habitat and its ocellar organisation is slightly different from *C. bicolor*. Majority of the ocellar rhabdoms in *C. fortis* were composed of three or four retinular cells, with some retinula cells contributing microvilli in one or more orientations (Fig. 5; Fig. 6). Thus, the anatomical results suggest that some but not all retinula cells of *C. fortis* are likely to detect changes in polarisation pattern. Behavioural and physiological evidence is required in this species to identify the extent to which *C. fortis* uses the pattern of polarised skylight with its ocelli.

Among the three species, the most unexpected and unusual ocellar organisation was seen in *M. bagoti.* The rhabdoms in this species formed a pentagonal and hexagonal network forming an open rhabdom (Fig. 5; Fig. 6), which is unlike in any other ant or hymenopteran ocelli that have been studied to date (Zeil et al. 2014). Their ocellar retina resembles that of the Bibionid flies, *Dilophus febrilis* (Wunderer et al. 1988), Flesh flies, *Boettcherisca peregrine* (Toh et al. 1971), and the Hover fly, *Eristalis tenax* (Ribi and Zeil 2018). In these four species, each retinula cell contributed microvilli in more than one orientation making their ocelli unsuitable for measuring changes in the pattern of polarised skylight. Behavioural evidence in *M. bagoti* suggests that they use the ocelli to derive celestial compass information, though the specific nature of these cues in unknown (Schwarz et al. 2011a). Ocellar spectral sensitivity in *M. bagoti* is not yet known but it is a possibility that *M. bagoti* uses their ocelli to access spectral cues to derive compass information (Rossel and Wehner 1984).

Physiology

In this part of my thesis, the aim was to measure the contrast sensitivity and the spatial resolving power of the ocelli in four *Myrmecia* ant species and in *Apis mellifera*. However, over the course of my study, it became apparent that it was difficult to obtain these measurements due to certain unexpected, yet exciting results. I found that the amplitude of the PERG response from the ocellar second order neurons in nocturnal *M. midas* and diurnal-crepuscular *M. tarsata* was significantly lower ($E^{-}O^{+}$; Fig. 8a,b, right column) when the ocelli alone were exposed to the visual stimuli in comparison to when both the visual systems were exposed to the stimuli ($E^{+}O^{+}$; Fig. 8a,b, left column). Due to this, the responses could not be quantitatively analysed to measure the previously

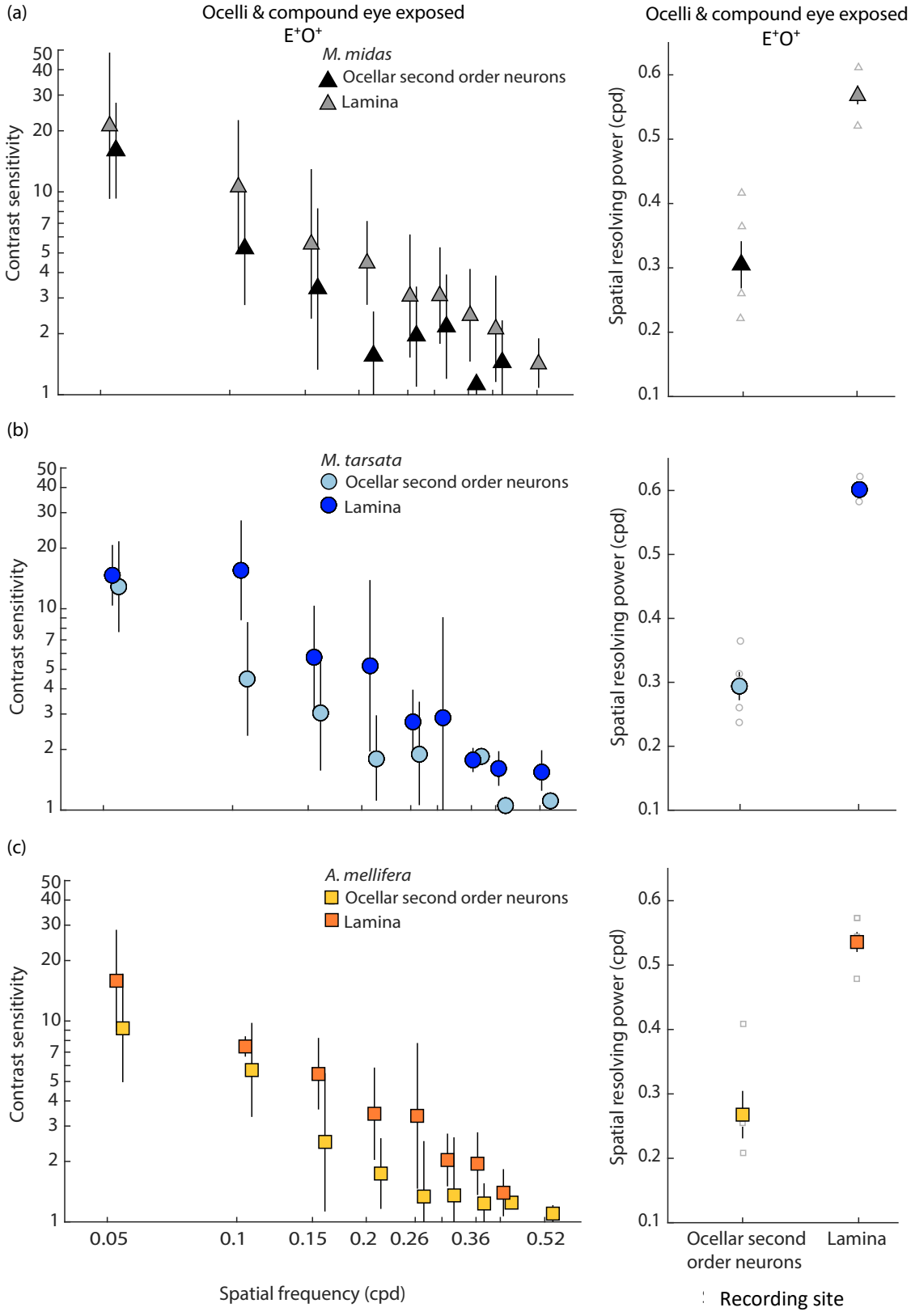

Figure 9. Contrast sensitivity function and spatial resolving power is higher in lamina than in the ocellar second order neurons of *M. midas*, *M. tarsata* and *A. mellifera*. Left panel: Each data point is the mean contrast sensitivity of all individuals of the particular species at the corresponding spatial frequency from a particular recording site. The error bars show 95% confidence intervals. (n=5) Right panel: Each coloured data point is the mean spatial resolving power of all individuals of

a particular species at 95% contrast from a particular recording site. Error bars show standard error. Grey outlined data points are individuals of a particular species. (n=5) Contrast sensitivity and spatial resolving power at two recording sites for (**a**) *M. midas,* (**b**) *M. tarsata* and **(c)** *A. mellifera* when both ocelli and compound eye are exposed to the visual stimuli. (Contrast sensitivity function and spatial resolving power of compound eye from *M. tarsata* and *M. midas* taken from Ogawa et al 2019. Contrast sensitivity function and spatial resolving power of compound eye from *A. mellifera*: unpublished data)

mentioned visual properties of the ocelli. To identify if an insect with a much larger median ocellus (Table 2) than the *Myrmecia* ant species and with a different mode of locomotion (flight) would produce similar results, I repeated the aforementioned experiments in the ocelli of *A. mellifera* (Fig. 8c). I found that in *M. midas*, *M. tarsata* and *A. mellifera* regardless of the ocellar diameter, time of activity and the mode of locomotion, the amplitude of the PERG response from the ocellar second order neurons was too low to be quantified when the ocelli alone were exposed to the visual stimuli ($E^{-}O^{+}$; Fig. 8, right panel).

There are two potential reasons for the low amplitude response of the ocellar second order neurons in *M. midas*, *M. tarsata*, and *A. mellifera*. One is that the compound eyes contribute significantly to the ocellar second order neurons which is distinct when we compare the responses of covered and uncovered compound eyes (Fig. 8). The neural architecture may explain some of this. The ocellar second order neurons in *A. mellifera* consist of large neurons (L-neurons) some of which lie in close proximity to the descending interneurons and are in intimate contact with one another (Guy et al. 1979). These descending neurons receive input from the compound eyes. Furthermore, some descending neurons send collaterals to the ocellar tract that contains these second order neurons (Guy et al. 1979). Anatomical and electrophysiological studies have shown similar structures in locusts (Simmons 2002), and flies (Strausfeld and Bassemir 1985; Parsons et al. 2006, 2010). The scale of the compound eye contribution to the ocellar second order neurons in all three species was however unexpectedly high. Hence, I compared the contrast sensitivity functions and the spatial resolving power of ocellar second order neurons and that of the compound eye second order neurons i.e., the lamina (*Myrmecia* ants: (Ogawa et al. 2019), *A. mellifera*: unpublished data) when both the ocelli and the compound eyes were exposed to the visual stimuli (Fig. 9). As expected, the contrast sensitivities and the spatial resolving power when recorded from the lamina was significantly higher in all three species when compared to ocellar second order neurons (Table 7 and 8, p-values $<<0.01$ in all species for both contrast sensitivity and spatial resolving power by Tukey post hoc test). This is most likely because the signal from the compound eyes reaches the ocellar second order neurons via the descending order neurons and hence is not conserved. The second possibility for the low amplitude response is that the ocellar response may be weakened when the compound eye is covered.

To be certain of this, an additional experiment of recording from ocellar second order neurons with the compound eye exposed and ocelli covered (E^+O^-) is required. If the amplitude, in this case, is similar to when both compound eyes and ocelli were stimulated E^+O^+ (Fig. 8, left column) then I can be certain that my present results (Fig. 8, left column) were responses from the compound eye. If the amplitude is intermediate between responses of E^+O^+ (Fig. 8, left column) and E^-O^+ (Fig. 8, right column) then this will help identify the contribution of the ocelli. Carrying out this additional experiment was beyond the scope of the duration of this thesis, but I plan to do so in the coming months.

When both the compound eyes and the ocelli were exposed to the visual stimuli, the contrast sensitivities and the spatial resolving power of the ocellar second order neurons in all five species were quantifiable, most likely due to the large input from the compound eyes. Under this condition, I found that the maximum contrast sensitivity of the ocellar second order neurons was highest in *M. midas* at 16 (6.3% contrast) and lowest in *A. mellifera* at 9.2 (10.8% contrast) (Table 2). However, the maximum contrast sensitivities were not significantly different between the five species (Table 3). Additionally, the contrast sensitivity functions were significantly different between the five species but the difference in the mode of locomotion did not explain this difference (Table 4). Nocturnal *Myrmecia* ants as previously described have wider ocellar rhabdoms, larger ocelli (Narendra and Ribi 2017) and have more and larger facets in their compound eyes (Ogawa et al. 2019) compared to the diurnal ants indicating that their ocellar second order neurons might have higher contrast sensitivities. However, among the ants, the time of activity did not explain the difference in contrast sensitivity functions between the four species (Table 5). This difference in contrast sensitivity functions is most likely caused by the large difference in contrast sensitivities between diurnal-crepuscular *M. gulosa* and nocturnal *M. pyriformis* at the intermediate spatial frequencies 0.1cpd and 0.15 cpd (Fig. 7). The anatomical characteristics of the visual system in diurnal-crepuscular *M. gulosa* is yet to be described, and hence it is unclear why the difference in contrast sensitivities exists. However, diurnal-crepuscular *M. tarsata* had more photoreceptors in its ocellar retina than the nocturnal *M. pyriformis* (Narendra and Ribi 2017), which can increase the sensitivity of the eye (Horridge 1977). Assuming the anatomical characteristics of diurnal-crepuscular *M. gulosa* is similar to that of diurnal-crepuscular *M. tarsata,* the difference in number of photoreceptors may explain the difference in contrast sensitivities.

The spatial resolving power of the ocellar second order neurons when both the compound eyes and the ocelli were exposed to the visual stimuli was not significantly different between the five species (Table 6). I suggest one reason for this. It is known that large number of photoreceptors

converge onto very few second-order interneurons in various species. For instance, in honeybees each photoreceptor repeatedly contacts a subset of eight second-order neurons resulting in a convergence ratio of 100:1 (Toh and Kuwabara 1974), without any reciprocal synapses between photoreceptors (Guy et al. 1979). High convergence ratios are also seen in locusts (Goodman and Williams 1976; Goodman et al. 1979), dragonflies (Patterson and Chappell 1980; Mizunami 1995; Berry et al. 2006), and cockroaches (Weber and Renner 1976; Mizunami 1995). If the number of second-order neurons in all four species of *Myrmecia* ants is similar to their hymenopteran counterpart *A. mellifera*, resulting in high and similar convergence ratios, it may not be surprising if the spatial resolving power does not vary between species, consistent with my results. This suggests that the fine-detail discrimination ability of the ocellar second order neurons is similar in all five species.

In the present study, I stimulated the median ocellus alone and recorded from the ocellar second order neurons which have inputs from both the median and lateral ocelli (e.g., Hung and Ibbotson 2014; Ribi and Zeil 2017). While the honeybees appear to have non-overlapping visual fields between the median and lateral ocelli (e.g., Hung and Ibbotson 2014; Ribi et al. 2011), in some species the visual fields overlap significantly (e.g., *Euglossa imperialis* (Taylor et al. 2016)). Therefore, it would be interesting to record from the ocellar second order neurons while stimulating both the lateral and median ocelli simultaneously and compare the results with my current findings.

Conclusion

This thesis reveals two exciting and unanticipated findings. First, the unusual rhabdom arrangement in the ocelli of *M. bagoti* consisting of open rhabdoms which has never been identified in the ocelli of any hymenopteran species to date. Second, the significantly high contribution of the compound eyes to the ocellar second order neurons when both ocelli and compound eyes were exposed to the visual stimuli. The anatomical analysis in this thesis suggests that in order to orient and navigate towards a goal, the desert ants used in this study seem to have adapted their ocellar anatomy to their respective habitats. Both species of *Cataglyphis* that live in saltpans or in urban regions in the Tunisian deserts have the anatomical substrate in the ocelli to detect changes in the polarisation pattern. In contrast, *Melophorus bagoti* that navigates in cluttered landscapes do not have the anatomical substrate in the ocelli to detect changes in the polarisation pattern. My physiological analysis in *Myrmecia* ants shows that the ocellar second order neurons had a low amplitude response to visual stimuli when the ocelli alone were stimulated, and this response might be mediated by the compound eyes. Hence, the spatial resolving power and the contrast sensitivity of the ocelli remains a mystery.

References

Armington JC, Adolph AR (1990) Local pattern electroretinograms and ganglion cell activity in the turtle eye. Int J Neurosci 50:1–11. doi: 10.3109/00207459008987152

Bach M, Hawlina M, Holder GE, et al (2000) Standard for pattern electroretinography. International Society for Clinical Electrophysiology of Vision. Doc Ophthalmol 101:11–18

Berry R, Stange G, Olberg R, Van Kleef J (2006) The mapping of visual space by identified large second-order neurons in the dragonfly median ocellus. J Comp Physiol A Neuroethol Sensory, Neural, Behav Physiol 192:1105–1123. doi: 10.1007/s00359-006-0142-5

Berry R, Van Kleef J, Stange G (2007a) The mapping of visual space by dragonfly lateral ocelli. J Comp Physiol A Neuroethol Sensory, Neural, Behav Physiol 193:495–513. doi: 10.1007/s00359-006-0204-8

Berry RP, Warrant EJ, Stange G (2007b) Form vision in the insect dorsal ocelli: An anatomical and optical analysis of the locust ocelli. Vision Res 47:1382–1393. doi: 10.1016/j.visres.2007.01.020

Cornwell PB (1955) The functions of the ocelli of *Calliphora* (Diptera) and *Locusta* (Orthoptera). J Exp Biol 32:217

Eaton JL, Tignor KR, Holtzman GI (1983) Role of moth ocelli in timing flight initiation at dusk. Physiol Entomol 8:371–375. doi: 10.1111/j.1365-3032.1983.tb00370.x

Fent K (1986) Polarized skylight orientation in the desert ant *Cataglyphis*. J Comp Physiol A 158:145–150. doi: 10.1007/BF01338557

Fent K, Wehner R (1985) Ocelli: A celestial compass in the desert ant *Cataglyphis*. Science 228:192–194. doi: 10.1126/science.228.4696.192

Freas CA, Narendra A, Cheng K (2017) Compass cues used by a nocturnal bull ant, *Myrmecia midas*. J Exp Biol 220:1578–1585. doi: 10.1242/jeb.152967

Ghim MM, Hodos W (2006) Spatial contrast sensitivity of birds. J Comp Physiol A Neuroethol Sensory, Neural, Behav Physiol 192:523–534. doi: 10.1007/s00359-005-0090-5

Goodman C, Williams J (1976) Anatomy of the ocellar interneurons of acridid grasshoppers. Cell Tissue Res 225:203–225

Goodman L, Mobbs P, Kirkham JB (1979) The fine structure of the ocelli of *Schistocerca gregaria*. Cell Tissue Res 196:487–510. doi: 10.1007/bf00234742

Gould JL (1975) Honeybee recruitment : The dance-language controversy. Science 189:685–693

Greiner B, Narendra A, Reid SF, et al (2007) Eye structure correlates with distinct foraging-bout timing in primitive ants. Curr Biol 17:879–880. doi: 10.1016/j.cub.2007.08.015

Guy RG, Goodman LJ, Mobbs PG (1979) Visual interneurons in the bee brain: Synaptic organisation and transmission by graded potentials. J Comp Physiol A 134:253–264. doi: 10.1007/BF00610399

Horridge GA (1977) The compound eye of insects. Sci Am 237:108–120. doi: 10.1038/scientificamerican0777-108

Hu KG, Stark WS (1980) The roles of *Drosophila* ocelli and compound eyes in phototaxis. J Comp Physiol A 135:85–95. doi: 10.1007/BF00660183

Hung Y-S, Ibbotson MR (2014) Ocellar structure and neural innervation in the honeybee. Front Neuroanat 8:1–11. doi: 10.3389/fnana.2014.00006

Kalmus H (1945) Correlations between flight and vision, and particularly between wings and ocelli, in insects. Proc R Entomol Soc London Ser A, Gen Entomol 20:84–96. doi: 10.1111/j.1365-3032.1945.tb01072.x

Kral K (1979) Neuronal connections in the ocellus of the wasp (*Paravespula vulgaris L.*). Cell Tissue Res 203:161–171. doi: 10.1007/BF00234335

Land MF (2002) Visual acuity in insects. Annu Rev Entomol 42:147–177. doi: 10.1146/annurev.ento.42.1.147

Lazzari CR, Reiseman CE, Insausti TC (1998) The role of the ocelli in the phototactic behaviour of the haematophagous bug *Triatoma infestans*. J Insect Physiol 44:1159–1162. doi: 10.1016/S0022-1910(98)00080-8

Mizunami M (1995) Information processing in the insect ocellar system: comparative approaches to the evolution of visual processing and neural circuits. Adv In Insect Phys 25:151–152. doi: 10.1016/S0065-2806(08)60065-X

Mote MI, Wehner R (1980) Functional characteristics of photoreceptors in the compound eye and ocellus of the desert ant, *Cataglyphis bicolor*. J Comp Physiol A 137:63–71. doi: 10.1007/BF00656918

Narendra A, Ramirez-Esquivel F, Ribi WA (2016) Compound eye and ocellar structure for walking and flying modes of locomotion in the Australian ant, *Camponotus consobrinus*. Sci Rep 6:1–10. doi: 10.1038/srep22331

Narendra A, Reid SF, Greiner B, et al (2011) Caste-specific visual adaptations to distinct daily activity schedules in Australian *Myrmecia* ants. Proc R Soc B Biol Sci 278:1141–1149. doi: 10.1098/rspb.2010.1378

Narendra A, Reid SF, Hemmi JM (2010) The twilight zone: Ambient light levels trigger activity in primitive ants. Proc R Soc B Biol Sci 277:1531–1538. doi: 10.1098/rspb.2009.2324

Narendra A, Ribi WA (2017) Ocellar structure is driven by the mode of locomotion and activity time in *Myrmecia* ants . J Exp Biol 220:4383–4390. doi: 10.1242/jeb.159392

Ogawa Y, Ryan LA, Palavalli-Nettimi R, et al (2019) Spatial resolving power and contrast sensitivity are adapted for ambient light conditions in Australian *Myrmecia* ants. Front Ecol Evol 7:1–10. doi: 10.3389/fevo.2019.00018

Palavalli-Nettimi R, Ogawa Y, Ryan LA, et al (2019) Miniaturisation reduces contrast sensitivity and spatial resolving power in ants. J Exp Biol jeb.203018. doi: 10.1242/jeb.203018

Parsons MM, Krapp HG, Laughlin SB (2006) A motion-sensitive neurone responds to signals from the two visual systems of the blowfly, the compound eyes and ocelli. J Exp Biol 209:4464–4474. doi: 10.1242/jeb.02560

Parsons MM, Krapp HG, Laughlin SB (2010) Sensor fusion in identified visual interneurons. Curr Biol 20:624–628. doi: 10.1016/j.cub.2010.01.064

Patterson JA, Chappell RL (1980) Intracellular responses of procion filled cells and whole nerve cobalt impregnation in the dragonfly median ocellus. J Comp Physiol A 139:25–39. doi: 10.1007/BF00666192

Penmetcha B, Ogawa Y, Ribi W, Narendra A. Ocellar structure in African and Australian desert ants. J Comp Physiol A, *in review*, *submitted:2019*

Porciatti V (2007) The mouse pattern electroretinogram. Doc Ophthalmol 115:145–153. doi: 10.1007/s10633-007-9059-8

Ribi W, Warrant E, Zeil J (2011) The organization of honeybee ocelli: Regional specializations and rhabdom arrangements. Arthropod Struct Dev 40:509–520. doi: 10.1016/j.asd.2011.06.004

Ribi W, Zeil J (2017) Three-dimensional visualization of ocellar interneurons of the orchid bee *Euglossa imperialis* using micro X-ray computed tomography. J Comp Neurol 525:3581–3595. doi: 10.1002/cne.24260

Ribi W, Zeil J (2018) Diversity and common themes in the organization of ocelli in Hymenoptera,

Odonata and Diptera. J Comp Physiol A Neuroethol Sensory, Neural, Behav Physiol 204:505–517. doi: 10.1007/s00359-018-1258-0

Rossel S, Wehner R (1984) Celestial orientation in bees: the use of spectral cues. J Comp Physiol A 155:605–613. doi: 10.1007/BF00610846

Ryan LA, Hemmi JM, Collin SP, Hart NS (2017) Electrophysiological measures of temporal resolution, contrast sensitivity and spatial resolving power in sharks. J Comp Physiol A Neuroethol Sensory, Neural, Behav Physiol 203:197–210. doi: 10.1007/s00359-017-1154-z

Schindelin J, Arganda-Carreras I, Frise E, et al (2012) Fiji: an open-source platform for biological-image analysis. Nat Methods 9:676–82. doi: 10.1038/nmeth.2019

Schricker B (1965) Die Orientierung der Honigbiene in der Dämmerung. Z Vgl Physiol 49:420–458. doi: 10.1007/bf00298112

Schuppe H, Hengstenberg R (1993) Optical properties of the ocelli of *Calliphora erythrocephala* and their role in the dorsal light response. J Comp Physiol A 173:143–149. doi: 10.1007/BF00192973

Schwarz S, Albert L, Wystrach A, Cheng K (2011a) Ocelli contribute to the encoding of celestial compass information in the Australian desert ant *Melophorus bagoti*. J Exp Biol 214:901–906. doi: 10.1242/jeb.049262

Schwarz S, Wystrach A, Cheng K (2011b) A new navigational mechanism mediated by ant ocelli. Biol Lett 7:856–858. doi: 10.1098/rsbl.2011.0489

Sheehan ZBV, Kamhi JF, Seid MA, Narendra A (2019) Differential investment in brain regions for a diurnal and nocturnal lifestyle in Australian *Myrmecia* ants. J Comp Neurol 1–17. doi: 10.1002/cne.24617

Simmons PJ (2002) Signal processing in a simple visual system: The locust ocellar system and its synapses. Microsc Res Tech 56:270–280. doi: 10.1002/jemt.10030

Somanathan H, Kelber A, Borges RM, et al (2009a) Visual ecology of Indian carpenter bees II: Adaptations of eyes and ocelli to nocturnal and diurnal lifestyles. J Comp Physiol A Neuroethol Sensory, Neural, Behav Physiol 195:571–583. doi: 10.1007/s00359-009-0432-9

Somanathan H, Warrant EJ, Borges RM, et al (2009b) Resolution and sensitivity of the eyes of the Asian honeybees *Apis florea*, *Apis cerana* and *Apis dorsata*. J Exp Biol 212:2448–2453. doi: 10.1242/jeb.031484

Sprint MM, Eaton JL (1987) Flight behavior of normal and anocellate cabbage loopers (Lepidoptera: Noctuidae). Ann Entomol Soc Am 80:468–471. doi: 10.1093/aesa/80.4.468

Stange G, Stowe S, Chahl JS, Massaro A (2002) Anisotropic imaging in the dragonfly median ocellus: A matched filter for horizon detection. J Comp Physiol A Neuroethol Sensory, Neural, Behav Physiol 188:455–467. doi: 10.1007/s00359-002-0317-7

Strausfeld NJ, Bassemir UK (1985) Lobula plate and ocellar interneurons converge onto a cluster of descending neurons leading to neck and leg motor neuropil in *Calliphora erythrocephala*. Cell Tissue Res 240:617–640. doi: 10.1007/BF00216351

Taylor GJ, Ribi WA, Bech M, et al (2016) The dual function of Orchid bee ocelli as revealed by X-ray microtomography. Curr Biol 26:1319–1324. doi: 10.1016/j.cub.2016.03.038

Toh Y, Kuwabara M (1974) Fine structure of the dorsal ocellus of the worker honeybee. J Morphol 143:285–305. doi: 10.1002/jmor.1051430304

Toh Y, Tominaga Y, Kuwabara M (1971) The fine structure of the dorsal ocellus of the fleshfly. J Electron Microsc (Tokyo) 20:56–66. doi: 10.1093/oxfordjournals.jmicro.a049760

van Kleef J, James AC, Stange G (2005) A spatiotemporal white noise analysis of photoreceptor responses to UV and green light in the dragonfly median ocellus. J Gen Physiol 126:481–497.

doi: 10.1085/jgp.200509319
Warrant EJ, Kelber A, Wallén R, Wcislo WT (2006) Ocellar optics in nocturnal and diurnal bees and wasps. Arthropod Struct Dev 35:293–305. doi: 10.1016/j.asd.2006.08.012
Weber G, Renner M (1976) The ocellus of the cockroach, *Periplaneta americana* (Blattariae) - Receptory area. Cell Tissue Res 168:209–222. doi: 10.1007/BF00215878
Wehrhahn C (1984) Ocellar vision and orientation in flies. Proc R Soc London Ser B Biol Sci 222:409–411. doi: 10.1098/rspb.1984.0073
Weiser MD, Kaspari M (2006) Ecological morphospace of New World ants. Ecol Entomol 31:131–142. doi: 10.1111/j.0307-6946.2006.00759.x
Wellington W (1974) Bumblebee ocelli and navigation at dusk. Science 183:551–552. doi: 10.1126/science.183.4124.551
Wilby D, Aarts T, Tichit P, et al (2018) Using micro-CT techniques to explore the role of sex and hair in the functional morphology of bumblebee (Bombus terrestris) ocelli. bioRxiv 433979. doi: 10.1101/433979
Wilson M (1978) The functional organisation of locust ocelli. J Comp Physiol A 124:297–316. doi: 10.1007/BF00661380
Wunderer H, Weber G, Seifert P (1988) The fine structure of the dorsal ocelli in the male bibionid fly. Tissue Cell 20:145–155. doi: 10.1016/0040-8166(88)90014-6
Zeil J, Ribi WA, Narendra A (2014) Polarization vision in ants, bees and wasps. In: Polarized Light and Polarization Vision in Animal Sciences, Second Edition. pp 41–60